Pump–probe spectra of linear molecular aggregates: Effect of exciton–exciton interaction and higher molecular levels

Gediminas Juzeliūnas
Abteilung Theoretische Physik, Universität Ulm, 89069 Ulm, Germany
and Institute of Theoretical Physics and Astronomy, A. Goštauto 12, Vilnius 2600, Lithuania

Peter Reineker
Abteilung Theoretische Physik, Universität Ulm, 89069 Ulm, Germany

(Received 4 March 1998; accepted 9 July 1998)

The paper considers the differential pump–probe spectra due to excitons in linear molecular aggregates taking into account simultaneously effects of both exciton–exciton interaction and higher molecular levels. The theoretical analysis, carried out in terms of the Green function technique, provides analytical expressions for the line shape of the pump–probe spectrum valid for an arbitrary number N of molecules forming the aggregate. Furthermore, the theory can accommodate any number of molecular states with higher energies. This includes, *inter alia*, the most common situation in which the higher lying states form a dense set of sublevels of electronic, vibrational, etc. origin. It has been demonstrated that incorporation of such higher molecular levels introduces widths to biexciton peaks formed below the two-exciton continuum. In addition, the indirect interaction between the excitons via the higher molecular levels can facilitate formation of a biexciton at lower than usual values of the direct exciton–exciton coupling γ, in extreme cases even for negative γ values characterizing repulsion rather than attraction between the excitons. On the other hand, in the region around the exciton band-edge, the differential spectrum can be described reasonably well in terms of the model of noninteracting excitons for a wide range of parameters of the system, subject to the replacement of an actual number of molecules per aggregate N by the effective one N_{eff}. The latter N_{eff} is shown to be influenced both by the direct coupling between the excitons and also by the indirect coupling via the higher molecular levels. © *1998 American Institute of Physics.* [S0021-9606(98)70638-5]

I. INTRODUCTION

Optical properties of molecular aggregates due to the transition between the ground electronic and the excited one-exciton states have been a subject of interest over many years.[1–8] However, only in the past decade more attention has been drawn to the nonlinear optical properties of such systems involving quantum states with more than one exciton per aggregate.[9–21] The interest was motivated, to a considerable degree, by the application of the time-resolved pump–probe spectroscopy in studying the molecular aggregates in organic[22–29] and biological[30,31] systems. In such experiments, a blue shift has been observed for the excited-state absorption of one-dimensional *J*-aggregates of pseudoisocyanine dye[22–29] and of complexes of the bacteriochlorophyll (BChl) molecules.[30,31] The effect has been explained on the basis of exciton-origin of the absorption lines, analyzing the one- to two-exciton transition in the molecular aggregates.[9,10,12–14,16,20,24,31] The comparison of the theory with the pump–probe experiments provides information on the delocalization lengths of excitons in molecular aggregates,[10] the degree of the intersite correlation of the inhomogeneous broadening in aggregates,[13,14] as well as other characteristics of the systems.[14,16,21] It is noteworthy that in most of the previous studies, such as in Refs. 9, 11–14, 16–18, excitons have been considered as noninteracting Paulions, and the influences of higher molecular levels have been neglected.

Recently the effects of the exciton–exciton interaction on the (two color) pump–probe spectra has been considered for molecular aggregates with linear[32–35] and circular[35] geometries. The analysis has been carried out in terms of two-particle Green functions adopting the continuum limit for the states forming the exciton band.[33,34] To take into account the finite size of the aggregates, both numerical simulations of the pump–probe spectra have been accomplished[32–34] and explicit analysis of the transition dipoles has been performed[35] for transitions between the one- and two-exciton states. The numerical calculations[33,34] have shown that the differential spectrum can experience significant changes if the strength of the exciton–exciton coupling is close to a critical value corresponding to the onset of biexciton formation below the band of dissociated two-exciton states. It is noteworthy that the calculated pump–probe spectrum[33,34] has appeared to be almost independent of the magnitude of the exciton–exciton coupling γ if the latter does not exceed a critical value γ_{crit}. This can be understood from the analysis of the dipole moments for the optical transition between the one- and two-exciton manifold[35] showing that the exciton–exciton interaction can be taken into account in an effective manner through the replacement of the actual number N of

molecules forming the aggregate by an effective number $N_{\rm eff}$ (with $|N_{\rm eff}-N|\ll N$ if γ is away from $\gamma_{\rm crit}$). In other investigations,[15,36] the two-photon absorption[15] and the pump–probe[36] spectra have been considered for noninteracting excitons in large molecular chains of three-level molecules. A similar chain of three level molecules has been also treated in a classic paper by Merrifield,[37] yet the analysis has been restricted to the stationary two-quantum excited states, no specific spectra (two-photon, pump–probe, etc.) being considered.

In the present paper we shall examine jointly the effects of the exciton–exciton interaction and the higher molecular levels on the differential pump–probe spectrum of one-dimensional molecular aggregates. The theoretical analysis carried out in terms of the Green function technique, is valid for an arbitrary number N of molecules forming the aggregate and accommodates any number of molecular states with higher energies as well. This includes, *inter alia*, the most common situation in which the higher-lying states are characterized by a dense set of sublevels of electronic, vibrational, etc. origin. In such a case the higher molecular levels play the role of a dissipative system that quenches pairs of lower lying excitons, thus making the exciton–exciton annihilation an irreversible process, as usually observed in experiments.[38] In the spectroscopic context, the inclusion of such a dissipative system introduces some widths to the biexciton levels formed below the two-exciton continuum. In addition, the indirect interaction between the excitons via the higher molecular levels can facilitate the formation of a biexciton at lower than usual values of the direct exciton–exciton coupling γ, in extreme cases even for negative γ values characterizing repulsion rather than attraction between the excitons. On the other hand, in the region around the exciton band-edge, the differential spectrum can be described reasonably well in terms of the model of noninteracting excitons for a wide range of the parameters of the system, subject to the replacement of the actual number of molecules per aggregate[39] N by the effective one $N_{\rm eff}$, the latter $N_{\rm eff}$ being now influenced both by the direct coupling between the excitons and also the indirect coupling via the higher molecular levels. In this way, effects such as the blue shift of the exciton absorption band established originally for noninteracting excitons,[9,10,12–14] persist also within the present more complicated model.

The analysis is carried out through the following steps. In Sec. II, after defining the Hamiltonian, the Jordan–Wigner transformation[10,14,40–42] is applied to convert molecular electronic excitations with lower energy into fermions. Next we separate the ''center of mass'' of the two Fermi-excitons from their relative motion via the introduction of operators for the creation and annihilation of exciton pairs. This allows us to avoid difficulties in counting the two-exciton states. Such difficulties can arise if one separates the ''center of mass'' from the relative motion in a usual way[14,37,43,44] using the original (paulion) representation for the two-exciton states. For instance, the cases with even and odd N require separate analysis[15,33] even for the case of noninteracting excitons.[14] Inclusion of the exciton–exciton interaction (as well as the higher molecular levels) adds additional difficulties if one is interested not only in biexcitons[43,44] (i.e., localized states for the relative motion of two excitons), but also in the dissociated two-exciton states at finite N. In fact, one can choose readily incorrect boundary conditions for the relative motion of the two excitons (subsequently affecting the eigenvalue spectrum of the dissociated two-exciton states), as discussed in detail recently.[35] It is noteworthy that the present approach does not face all these difficulties, as the fermionization carried out before the separation into the ''center of mass'' and the relative motion solves the problems automatically. In Sec. III the line shape of the excited-state absorption is presented through the two-particle Green functions. The latter Green functions are subsequently derived in terms of those for the free excitons, details of the derivation being placed in Appendix A. The summations emerging in the free-exciton Green functions are then explicitly calculated (in Appendix B) adapting a method suggested by Montrol[45] and Lakatos-Lindenberg *et al.*[46] in their studies of random walks on lattices. As a result, in Sec. IV one arrives at analytical expressions for the differential spectrum of the combined system containing interacting excitons and higher molecular excitations. The expressions are valid for any number of molecules N in the aggregate. Specific calculations are also presented in Sec. IV to illustrate the general theory. The concluding Sec. V summarizes the findings.

II. HAMILTONIAN

Consider a system of interacting molecular excitons coupled to higher excited molecular levels in a one-dimensional molecular aggregate. The Hamiltonian for such a system is

$$H=\sum_{n=1}^{N}\Big\{\varepsilon t_n^+ t_n - L(t_{n+1}^+ t_n + t_n^+ t_{n+1}) - \gamma t_n^+ t_{n+1}^+ t_{n+1} t_n + \sum_{\alpha}\big[\varepsilon_\alpha c_{n\alpha}^+ c_{n\alpha} + \chi_\alpha (c_{n\alpha}^+ + c_{(n+1)\alpha}^+) t_{n+1} t_n + \chi_\alpha^* t_n^+ t_{n+1}^+ (c_{n\alpha} + c_{(n+1)\alpha})\big]\Big\}, \tag{2.1}$$

where N is the number of molecules in the aggregate, t_n^+ (t_n) are Pauli operators for the creation (annihilation) of an electronic excitation at molecule n, ε being the excitation energy. Another set of operators $c_{n\alpha}^+$ and $c_{n\alpha}$ describes the creation and annihilation of molecular excitations with higher energies ($\varepsilon_\alpha > \varepsilon$), the summation over α covering molecular levels of interest. The Hamiltonian (2.1) incorporates (within nearest neighbor approximation) both the resonance transfer of the low-energy excitons between the molecules and their mutual coupling, where $(-L)$ and $(-\gamma)$ are the corresponding coupling constants. For higher molecular levels the resonance energy transfer is usually of much less importance and hence has been disregarded in the Hamiltonian (2.1). The two types of excitations interact via the annihilation of two low-energy excitons at neighboring sites, accompanied by the promotion of one of the two molecule to a higher excited level α, with χ_α being the coupling con-

stant; the Hermitian conjugate terms in the Hamiltonian (2.1) describe the opposite process. Finally, cyclic boundary conditions imply that

$$t_{N+1}\equiv t_1 \quad \text{and} \quad c_{(N+1)\alpha}=c_{1\alpha}, \tag{2.2}$$

together with analogous relationships for the creation operators. It is noteworthy that in contrast to a recent study by Knoester and Spano,[15] the Hamiltonian (2.1) incorporates the exciton–exciton coupling ($\gamma\neq 0$) and also can take into account an arbitrary number of higher molecular levels α. Specifically, the present model can describe the most common situation where the levels α comprise a dense set of higher molecular sublevels (of electronic, vibrational, etc. origin) in resonance with the two-exciton states. Note also some similarities between the present Hamiltonian and the one used in the theory of biphonons and Fermi resonance in the vibrational spectra of crystals.[47,48]

A. Fermionization

For the present purposes, it is sufficient to consider the Hilbert space comprising the quantum states with up to two low-lying excitons and up to one molecular excitation with higher energy. The operators, t_n^+ and t_n describing the former type of the quasiparticles obey mixed Fermi and Bose commutation relations known as the Pauli commutation relations.[10,14,41–43,49] Therefore the Pauli operators t_n^+ and t_n are not convenient when dealing with the states containing more than one exciton. To facilitate the analysis, we shall invoke the Jordan–Wigner transformation[10,14,17,40,41] converting the original Pauli operators into a set of operators a_n and a_n^+ obeying exact Fermi commutation relations, as

$$a_n=(-1)^{\sigma_n}t_n; \quad t_n=(-1)^{\sigma_n}a_n \tag{2.3}$$

$(n=1,2,\ldots,N)$, with

$$\sigma_n=\sum_{j=1}^{n-1} t_j^+ t_j=\sum_{j=1}^{n-1} a_j^+ a_j. \tag{2.4}$$

The operator a_n describes the annihilation of a Fermi-exciton at the site n, a_n^+ being the corresponding creation operator. Note that the other set of operators $c_{n\alpha}^+$ and $c_{n\alpha}$ does not require any fermionization, as our consideration is restricted to states with up to one molecular electronic excitation of this type. In fact, the present paper concentrates on pump–probe spectroscopy probing the excited-state manifold that contains a superposition of two Fermi-excitons and one higher molecular excitation. The states in which two or more molecules are promoted to higher excited levels, are characterized by much larger energies than those of two Fermi-excitons. Such states are not accessible via the pump–probe spectroscopy of interest due to detuning effects.

To represent the Hamiltonian (2.1) via the new operators, consider first the terms of the Hamiltonian that do not contain the Pauli operators belonging to the boundary sites N and $N+1$. Such nonboundary terms preserve their original form, i.e., one can simply change the letter t (referring to Pauli operators) into the letter a (denoting Fermi operators) in the corresponding terms of the Hamiltonian (2.1); this is a consequence of the one-dimensionality of the system along with the adopted nearest-neighbor approximation.[9,10,14,17,18,41,42] Consider now the boundary terms. The appropriate pair-operators featured in the Hamiltonian acquire now a phase factor $(-1)^q$, as presented in Ref. 41 analyzing a system of noninteracting excitons in one dimension, $t_{N+1}^+ t_N\equiv t_1^+ t_N=a_1^+ a_N(-1)^q$ and $t_N^+ t_{N+1}=a_N^+ a_1(-1)^q$, the operators $t_N^+ t_{N+1}^+$ and $t_{N+1}t_N$ transforming in a similar way. Here the parameter q can assume two different values; specifically, $q=0$ ($q=1$) in the case where the Hamiltonian H acts on the state-vector characterized by the odd (even) number of Fermi-excitons. To eliminate the phase factor, we shall introduce the Fermi operators a_{N+1} and a_{N+1}^+ related to a_1 and a_1^+ as follows:

$$a_{N+1}\equiv a_1(-1)^q; \quad a_{N+1}^+\equiv a_1^+(-1)^q. \tag{2.5}$$

Using condition (2.5), the whole Hamiltonian retains its original form (2.1) and can hence be represented as

$$H=H^{\text{ex}}+H^{\text{high}}+H^{\text{high-ex}}+H^{\text{ex-high}}, \tag{2.6}$$

with

$$H^{\text{ex}}=\sum_{n=1}^{N}[\varepsilon a_n^+ a_n-L(a_{n+1}^+ a_n+a_n^+ a_{n+1}) - \gamma a_n^+ a_{n+1}^+ a_{n+1}a_n], \tag{2.7}$$

$$H^{\text{high}}=\sum_{n=1}^{N}\sum_{\alpha}\varepsilon_\alpha c_{n\alpha}^+ c_{n\alpha}, \tag{2.8}$$

$$H^{\text{high-ex}}=\sum_{n=1}^{N}\sum_{\alpha}\chi_\alpha(c_{n\alpha}^+ + c_{(n+1)\alpha}^+)a_{n+1}a_n, \tag{2.9}$$

and

$$H^{\text{ex-high}}=\sum_{n=1}^{N}\sum_{\alpha}\chi_\alpha^* a_n^+ a_{n+1}^+(c_{n\alpha}+c_{(n+1)\alpha}), \tag{2.10}$$

where the factor $(-1)^q$ is hidden in the boundary condition (2.5) for the operators a_{N+1} and a_{N+1}^+. Condition (2.5) will lead to two different sets of the wave number values $\tilde{k}$ corresponding to states with an even and odd number of Fermi-excitons, as presented in Eq. (2.12) below. It is to be emphasized that parameter q can indeed be used to classify the eigenstates of the Hamiltonian H in which operators for the creation and annihilation of Fermi-excitons appear always in pairs.

The separation of the full Hamiltonian into the terms in Eq. (2.6), corresponds to the division of the full system into a subsystem of interacting Fermi-excitons and into that due to the higher molecular states; Both subsystems are characterized by their Hamiltonians H^{ex} and H^{high}, respectively. The remaining terms $H^{\text{high-ex}}$ and $H^{\text{ex-high}}$ describe the interaction between the two subsystems. The former operator $H^{\text{high-ex}}$ corresponds to processes involving the destruction of two Fermi-excitons accompanied by the promotion of the system to a higher molecular state, $H^{\text{ex-high}}$ being the Hermitian conjugated counterpart representing the opposite processes.

B. Transition into the momentum space

Next we shall transform the Fermi-operators into the momentum space,

$$b_{\tilde{k}}^{+}=N^{-1/2}\sum_{n=1}^{N} a_n^{+}e^{i\tilde{k}n};\quad a_n^{+}=N^{-1/2}\sum_{\tilde{k}} b_{\tilde{k}}^{+}e^{-i\tilde{k}n}, \tag{2.11}$$

where the boundary condition (2.5) provides the following set of $\tilde{k}$ values:

$$\tilde{k}=\pi(2j+q)/N, \tag{2.12}$$

the number j assumes N consecutive integer values, and the parameter q can again take one of the two values 0 or 1 depending on whether the exciton number in the system is odd ($q=0$) or even ($q=1$). Note that the tilde has been placed here over the wave number $\tilde{k}$ to reserve the usual lower case k for the wave number of the relative motion of two excitons introduced in Eqs. (2.15) and (2.16) below.

In terms of the new operators, the Hamiltonian for the exciton subsystem (2.7) reads

$$H^{\mathrm{ex}}=\sum_{\tilde{k}} E_{\tilde{k}}b_{\tilde{k}}^{+}b_{\tilde{k}}-\gamma\sum_{K} B_K^{+}B_K, \tag{2.13}$$

where

$$E_{\tilde{k}}=\varepsilon-2L\cos\tilde{k} \tag{2.14}$$

is the energy of a free Fermi-exciton. Here the coupling between the Fermi-excitons has been expressed via the auxiliary operators

$$B_K^{+}=N^{-1/2}\sum_{k} b_{K/2+k}^{+}b_{K/2-k}^{+}e^{ik};$$

$$B_K=N^{-1/2}\sum_{k} b_{K/2-k}b_{K/2+k}e^{-ik} \tag{2.15}$$

describing the creation and annihilations of exciton pairs at neighboring molecules, with

$$K=2\pi l/N;\quad k=\pi(2j-l+q)/N, \tag{2.16}$$

being, respectively, the wave number for the motion of the ''center of mass'' of the two excitons and that for their relative motion, l and j taking N consecutive integer values, and $q=0,1$ as in Eq. (2.12).

Transforming also the other set of creation and annihilation operators into the momentum space

$$C_{K,\alpha}^{+}=N^{-1/2}\sum_{n=1}^{N} c_{n,\alpha}^{+}e^{iKn};\quad c_{n,\alpha}^{+}=N^{-1/2}\sum_{K} C_{K,\alpha}^{+}e^{-iKn}, \tag{2.17}$$

the remaining components (2.8)–(2.10) of the Hamiltonian take the form

$$H^{\mathrm{high}}=\sum_{\alpha}\varepsilon_\alpha\sum_{K} C_{K,\alpha}^{+}C_{K,\alpha}, \tag{2.18}$$

$$H^{\text{high-ex}}=\sum_{K} 2\cos(K/2)\sum_{\alpha}\chi_\alpha C_{K,\alpha}^{+}B_K, \tag{2.19}$$

and

$$H^{\text{ex-high}}=\sum_{K} 2\cos(K/2)\sum_{\alpha}\chi_\alpha^{*}B_K^{+}C_{K,\alpha}, \tag{2.20}$$

with K as in Eq. (2.16).

C. Eigenstates

The eigenstates of the system split into the following manifolds:

(1) The electronic ground state $|g\rangle$ containing no Fermi-excitons and no higher molecular excitations, so that $a_n|g\rangle=c_{n,\alpha}|g\rangle=0$.

(2) One-exciton states containing one Fermi-exciton

$$|K\rangle=b_K^{+}|g\rangle, \tag{2.21}$$

where the wave vector K is as in Eq. (2.16); this corresponds to the case $q=0$ (the number of excitons is odd) in the general relation for the wave vector (2.12). Note that the higher-molecular levels are not yet involved, as at least two Fermi excitons are required for the coupling with the higher-excited states to come into play via the interaction operators (2.19) and (2.20).

(3) In what follows, we shall concentrate on the next set of the excited states representing superpositions between the states with two Fermi-excitons and one molecular excitation with higher energies ε_α; it is this manifold of the excited states to which the aggregate is promoted in the pump–probe experiments via the upward optical transitions from the one-exciton states. The pump–probe spectra will be treated by means of the Green function technique bypassing the explicit analysis of the eigenvalue problem for such a manifold.

III. LINE SHAPE OF THE EXCITED-STATE ABSORPTION

A. General

1. Dipole operator

The dipole operator, inducing the optical transitions within the aggregate, reads

$$M=M_{+}+M_{-}=\left(\mu^{*}J_{+}+\sum_{\alpha}\mu^{1\alpha}J_{+}^{1\alpha}\right)+\left(\mu J_{-}+\sum_{\alpha}\mu^{\alpha 1}J_{-}^{1\alpha}\right), \tag{3.1}$$

with

$$J_{+}=\sum_{n=1}^{N} t_n^{+}=\sum_{n=1}^{N}(-1)^{\sigma_n}a_n^{+};\quad J_{-}=(J_{+})^{+}, \tag{3.2}$$

$$J_{+}^{1\alpha}=\sum_{n=1}^{N} c_{n,\alpha}^{+}t_n=\sum_{n=1}^{N} c_{n,\alpha}^{+}(-1)^{\sigma_n}a_n;\quad J_{-}^{1\alpha}=(J_{+}^{1\alpha})^{+}. \tag{3.3}$$

Here the operator $J_{+}(J_{-})$ describes creation (annihilation) of Fermi-excitons by light, μ^{*} (μ) being the corresponding molecular transition dipole along the polarization of light. As discussed earlier,[9,10] such an operator acquires a many-

particle character after the fermionization due to the emerging factor $(-1)^{\sigma_n}$, the factor playing an important role in one- to two-exciton transitions. The operator $J_+^{1\alpha}$ describes the annihilation of a Fermi-exciton accompanied by the creation of an excitation with higher energy (i.e., promotion of the system from a low-lying excited state to a higher molecular level α), the operator $J_-^{1\alpha}$ represents the opposite process, $\mu^{1\alpha}$ and $\mu^{\alpha 1}$ being the corresponding transition dipoles along the polarization of light. For the present purposes the factor $(-1)^{\sigma_n}$ can be omitted in $J_+^{1\alpha}$, as we restrict ourselves to optical transitions originating from the quantum states with up to one Fermi-exciton.

In writing the above relationships, the transition dipoles of individual molecules are assumed to be parallel to each other. As a result, the index n is not featured in the quantities μ and $\mu^{1\alpha}$. Furthermore, the size of the aggregate is considered to be small as compared to the wavelength, so the retardation factors are not featured in the operators J_+ and $J_+^{1\alpha}$. Note also that the dipole operator (3.1) does not include the processes of direct creation or annihilation of the high-energy excitations: These transitions are characterized by energies that are much higher than the energy of Fermi-excitons, and hence do not contribute to the pump–probe spectrum in the exciton area of interest.

2. Line shape

Consider the line shape of optical absorption of the aggregate from a yet unspecified initial state $|\mathrm{in}\rangle$,

$$I^{\mathrm{in}}(E)=I_+^{\mathrm{in}}(E)-I_-^{\mathrm{in}}(E), \tag{3.4}$$

with

$$I_\pm^{\mathrm{in}}(E)=\sum_{\mathrm{fin}} |\langle \mathrm{fin}|M_\pm|\mathrm{in}\rangle|^2 \delta(E_{\mathrm{in}}-E_{\mathrm{fin}}\pm E), \tag{3.5}$$

where the summation is over all optically accessible final states $|\mathrm{fin}\rangle$, both initial and final states being eigenstates of the full Hamiltonian (2.19) with eigenenergies E_{in} and E_{fin}. The positive contribution $I_+^{\mathrm{in}}(E)$ represents the usual absorption involving the upward optical transitions in the aggregate. The negative contribution $I_-^{\mathrm{in}}(E)$ describes the induced emission that can be understood as the negative absorption due to the downward transitions in the aggregate. Subtracting from Eq. (3.5) the line shape of the ground-state absorption $I^g(E)$, one arrives at the differential pump–probe spectrum (associated with the optical transition from the one exciton state $|\mathrm{in}\rangle=|K\rangle$ to which the system is promoted by the initially applied pump-pulse),

$$\Delta I^K(E)=I_+^K(E)-I_-^K(E)-I^g(E), \tag{3.6}$$

where E denotes the energy of a probe photon. Such a differential spectrum is relevant to pump–probe experiments, see, e.g., Refs. 22–24, 30, 31.

Since $\delta(x)=\pi^{-1}\,\mathrm{Im}(x-is)^{-1}$ (with $s\to+0$), Eq. (3.5) may be rewritten in a form that is more convenient for the subsequent analysis,

$$I_\pm^{\mathrm{in}}(E)=\pi^{-1}\,\mathrm{Im}\sum_{\mathrm{fin}}\langle \mathrm{in}|M_\mp|\mathrm{fin}\rangle \times(E_{\mathrm{in}}\pm E-E_{\mathrm{fin}}-is)^{-1}\langle \mathrm{fin}|M_\pm|\mathrm{in}\rangle. \tag{3.7}$$

Note that the retention of a small (yet finite) quantity s makes it possible to introduce phenomenologically a finite homogeneous linewidth for the molecular spectral lines characterized by Lorentzian shapes. Furthermore, depending on experimental conditions, the finite s may represent other broadening effects, like an inhomogeneous segment distribution or laser pulse widths (for more details see, e.g., Ref. 36). In the simpliest case of optical transitions from the ground electronic state, one has $|\mathrm{in}\rangle=|g\rangle$ and $E_{\mathrm{in}}=E_g=0$, giving

$$I^g(E)=I_+^g(E)=\mathrm{Im}\,\frac{\pi^{-1}|\mu|^2N}{E-(\varepsilon-2L)-is}, \tag{3.8}$$

i.e., only upward transition to the one exciton state with $K=0$ contribute to the line shape $I^g(E)$.

3. Sum rule

We complete the subsection by writing a general sum rule obeyed by the absorption line shape (3.4),[9,10]

$$\int I^{\mathrm{in}}(E)dE=N|\mu|^2-\left(2|\mu|^2-\sum_\alpha |\mu^{1\alpha}|^2\right)m, \tag{3.9}$$

where m is the number of the excitons in the initial state, i.e., $m=0$ in the case of transitions from the ground electronic state ($|\mathrm{in}\rangle=|g\rangle$), and $m=1$ for transitions from one-exciton states ($|\mathrm{in}\rangle=|K\rangle$). In terms of the differential spectrum (3.6), the sum rule (3.9) reads

$$\int \Delta I^K(E)dE=-2|\mu|^2+\sum_\alpha |\mu^{1\alpha}|^2, \tag{3.10}$$

showing that the integral over the differential spectrum is determined by the transition dipoles μ and $\mu^{1\alpha}$ only. In other words, the integral (3.10) does not depend on other parameters of the system, such as the energies of resonance coupling $(-L)$ and the exciton–exciton interaction $(-\gamma)$, as well as the energy of the coupling between the Fermi-excitons and the higher molecular excitations (χ_α). It is noteworthy that the sum rule for the line shape $I^{\mathrm{in}}(E)$ has been originally derived analyzing a system of noninteracting excitons in one dimension.[9,10] Yet, its derivation is based only on the general commutation relations for the Pauli-operators entering the dipole operator (3.1), as well as on the assumption that the transition dipoles of individual molecules are parallel to each other. As a result, the sum rule (3.9) [or (3.10)] is applicable to a much wider range of molecular systems, including the one considered here, systems influenced by static disorder and phonons, and also systems with higher dimensions. The above sum-rules demonstrate that $|\int \Delta I^K(E)dE|/\int I^g(E)dE\sim 1/N$, i.e., for large aggregates $(N\gg 1)$ the integrated change of the absorption line shape is much smaller than the integrated line shape itself. This goes along with the pump–probe experiments on J-aggregates showing a blue-shift (with almost no bleaching) of the exciton J-band.[22–29] Previous theoretical analyses of the one- to two-exciton transition does indeed yield such a

blue shift,[9,10,12–14,34,36] the effect being retained in many cases in the present model incorporating both the exciton–exciton coupling and an arbitrary number of higher molecular levels, as will be demonstrated in Sec. IV.

B. Line shape for transitions from one-exciton states

In what follows, we shall concentrate on optical transitions from the one-exciton states $|K\rangle$. In such a situation, the contribution due to the induced emission reads

$$I_{-}^{K}(E)=\delta_{K,0}I_{+}^{g}(E), \tag{3.11}$$

where $I_{+}^{g}(E)$ is the line shape of ground-state absorption given by Eq. (3.8). The Kronecker delta reflects the fact that downward transitions to the ground electronic state ($|K\rangle \rightarrow|g\rangle$) are possible only from the optically active state with $K=0$. On the other hand, the line shape due to the upward transitions cannot be written in such a simple form, since the final eigenvectors $|\mathrm{fin}\rangle$ represent a complex superposition of the two-exciton states and the states containing one molecular excitation with higher energy. To bypass the explicit analysis of the state-vectors $|\mathrm{fin}\rangle$, we shall make use of the fact that they comprise a complete basis, and can thus be discarded from Eq. (3.7) to yield

$$I_{+}^{K}(E)=\pi^{-1}\ \mathrm{Im}\langle K|M_{-}GM_{+}|K\rangle, \tag{3.12}$$

where

$$G\equiv G(E+E_K)=[(E+E_K)-H-is]^{-1}\quad (s\rightarrow+0) \tag{3.13}$$

is the Green operator (corresponding to the Hamiltonian H), E_K being the energy of the initial one-exciton state, as given by Eq. (2.14) subject to the substitution $\tilde{k}\rightarrow K$.

In Appendix A, the Green operator G has been determined in terms of the Green operator for free excitons $G_{\mathrm{free}}^{\mathrm{ex}}$ invoking the projection operator technique. We shall substitute the results (A6) and (A14) for G into the line shape (3.12), subsequently exploiting Eqs. (3.1)–(3.3) for the dipole operators, as well as Eqs. (2.18)–(2.20) for the terms comprising the Hamiltonian. As a result, one arrives then at the following absorption line shape (These results will be discussed in detail in Sec. IV in connection with the representation of the differential pump–probe spectrum):

$$I_{+}^{K}(E)=I_{+\,\mathrm{free\text{-}ex}}^{K}(E)+I_{+\,\mathrm{int1}}^{K}(E)+I_{+\,\mathrm{int2}}^{K}(E)+I_{+\,\mathrm{high}}^{K}(E). \tag{3.14}$$

Here the constituent terms read

$$I_{+\,\mathrm{free\text{-}ex}}^{K}(E)=\pi^{-1}|\mu|^{2}\ \mathrm{Im}\langle K|J_{-}G_{\mathrm{free}}^{\mathrm{ex}}J_{+}|K\rangle, \tag{3.15}$$

$$I_{+\,\mathrm{int1}}^{K}(E)=\pi^{-1}|\mu|^{2}\ \mathrm{Im}\left[\frac{2La_K(\langle K|J_{-}G_{\mathrm{free}}^{\mathrm{ex}}B_K^{+}|g\rangle)^{2}}{1+2La_K\langle g|B_KG_{\mathrm{free}}^{\mathrm{ex}}B_K^{+}|g\rangle}\right], \tag{3.16}$$

$$I_{+\,\mathrm{int2}}^{K}(E)=\pi^{-1}\ \mathrm{Im}\left[\frac{\langle K|J_{-}G_{\mathrm{free}}^{\mathrm{ex}}B_K^{+}|g\rangle(\mu u_K-\mu^{*}\widetilde{u_K})+\langle g|B_KG_{\mathrm{free}}^{\mathrm{ex}}B_K^{+}|g\rangle u_K\tilde{u}_K}{1+2La_K\langle 0|B_KG_{\mathrm{free}}^{\mathrm{ex}}B_K^{+}|0\rangle}\right], \tag{3.17}$$

$$I_{+\,\mathrm{high}}^{K}(E)=\pi^{-1}\ \mathrm{Im}\sum_{\alpha}\ \frac{|\mu_{1\alpha}|^{2}}{E+E_K-\varepsilon_\alpha-is}, \tag{3.18}$$

with

$$u_K=\sum_{\alpha}\ \frac{2\chi_\alpha^{*}\mu_{1\alpha}\cos(K/2)}{E+E_K-\varepsilon_\alpha-is},$$

$$\widetilde{u_K}=\sum_{\alpha}\ \frac{2\chi_\alpha\mu_{\alpha1}\cos(K/2)}{E+E_K-\varepsilon_\alpha-is}, \tag{3.19}$$

and

$$a_K\equiv\gamma_K'(E)/2L=\gamma/2L$$
$$-4\cos^{2}(K/2)\sum_{\alpha}\ \frac{|\chi_\alpha|^{2}/2L}{E+E_K-\varepsilon_\alpha-is}, \tag{3.20}$$

where $\gamma_K'(E)$ has been defined by Eq. (A11), and the operator $G_{\mathrm{free}}^{\mathrm{ex}}$ is given by Eq. (A12) in Appendix A. The dimensionless parameter a_K contains contributions due to both the direct coupling between the Fermi-excitons $\gamma/2L$ and also the additional (indirect) coupling between the excitons via the the higher molecular levels. The latter indirect coupling is represented by the second term in Eq. (3.20).

Equations (3.14)–(3.18) define the absorption line shape in terms of the Green functions for free excitons, the latter functions are given explicitly by Eqs. (A16)–(A18) in Appendix A. In the following we shall concentrate on optical transitions from the one-exciton state with $K=0$. In fact, due to the $K=0$ selection rule, only such a state can be populated during the ground-state absorption of a photon from the pump pulse. As a result, the subsequent absorption of a probe photon does take place from this one-exciton state, as long as the aggregate does not undergo thermal transitions to other one-exciton levels with higher energies.[51] For $K=0$, the Green functions given by Eqs. (A16)–(A18) reduce to the following:

$$\langle 0|J_{-}G_{\mathrm{free}}^{\mathrm{ex}}J_{+}|0\rangle=-\frac{1}{2L}\frac{1}{p-1}[N-(p+1)S_0(p)], \tag{3.21}$$

$$\langle K|J_{-}G_{\mathrm{free}}^{\mathrm{ex}}B_0^{+}|0\rangle=\frac{i}{2L}[S_0(p)+S_1(p)], \tag{3.22}$$

$$\langle 0|B_0G_{\mathrm{free}}^{\mathrm{ex}}B_0^{+}|0\rangle=-\frac{1}{4L}[S_0(p)-S_2(p)], \tag{3.23}$$

with

$$S_n(p)=\frac{1}{N}\sum_{k}\ \frac{\exp(ikn)}{p-\cos k}, \tag{3.24}$$

and

$$p=(\varepsilon+2L-E+is)/4L. \tag{3.25}$$

The above summation $S_n(p)$ has the form of the familiar one-exciton Green function. In dealing with such functions, the summation over k is normally replaced by an integration (see, e.g., Refs. 14–16, 33, 34, 36, 44, 50) assuming that the number N is sufficiently large. To retain the effects of finite N, we shall make use of another method originally suggested by Montrol[45] and Lakatos-Lindenberg *et al.*[46] in their studies of random walk on lattices. Note that in the present situation the wave number k, characterizing the relative motion of the two excitons, can assume values different from those in Refs. 45 and 46. In fact, there are two possible sets of k given by Eq. (2.16) depending on a specific value of the full wave vector $K=2\pi l/N$ [with $q=1$ in Eq. (2.16), as we deal with the states containing even number of Fermi-excitons]. In the case of odd l, Eq. (2.16) yields a set of k values considered in Refs. 45 and 46. However for even l (e.g., for $l=K=0$), one arrives at another set in which the value $k=0$ does not appear. The summation (3.24) has been carried out in Appendix B for the present purposes. Using Eq. (B5), one finds for $K=0$,

$$S_n(p)=\frac{2}{b-b^{-1}}\,\frac{b^{-n}-b^{-(N-n)}}{1+b^{-N}}, \tag{3.26}$$

with

$$b=p+\sqrt{p^2-1},\quad b^{-1}=p-\sqrt{p^2-1}. \tag{3.27}$$

Equation (3.26) is an exact result valid for an arbitrary number N. It is instructive that the Green function (3.26) is not affected by the interchange $b\leftrightarrow b^{-1}$. In other words, the sign of the square root $\sqrt{p^2-1}$ can be reversed simultaneously both in b and b^{-1}. In Eq. (3.27) the specific sign of the square root has been chosen in such a way that $|b|>1$, if the energy E of a probe photon lies within the exciton zone or below $(E<\varepsilon+2L)$. This spectral area is most important for the optical absorption involving predominantly the lowest levels of the exciton band.[51] (If the energy E is situated above the exciton zone $E>\varepsilon+2L$, the sign of the square root is to be reversed in Eq. (3.27) to get $|b|>1$.) The choice $|b|>1$ allows us to neglect the term $b^{-(N-n)}$ in Eq. (3.26) at sufficiently large N. Note that for the energies lying within the exciton zone $\varepsilon-2L<E<\varepsilon+2L$, the limit of large N is achieved in the case where the linewidth s of the individual molecules exceeds considerably the distances between the exciton levels, $sN/4L|1-p^2|^{1/2}\gg 1$.

IV. ANALYSIS OF THE DIFFERENTIAL PUMP–PROBE SPECTRUM

Using Eq. (3.14) for the line shape $I_+^K(E)$, the differential spectrum (3.6) can be written as

$$\Delta I^K(E)=\Delta I^K_{\text{free-ex}}(E)+I^K_{+\,\text{int1}}(E)+I^K_{+\,\text{int2}}(E)+I^K_{+\,\text{high}}(E), \tag{4.1}$$

where both the induced emission and the ground-state absorption are now contained in the free-exciton term,

$$\Delta I^K_{\text{free-ex}}(E)=I^K_{+\,\text{free-ex}}(E)-I^K_-(E)-I_g(E). \tag{4.2}$$

In the case of $K=0$, the contribution $\Delta I^K_{\text{free-ex}}(E)$ and the term $I^K_{+\,\text{int1}}(E)$ read explicitly

$$\Delta I^0_{\text{free-ex}}(E)=\frac{|\mu|^2}{2\pi L}\,\text{Im}\,\frac{1}{(p-1)}\left(\frac{1+b^{-1}}{1-b^{-1}}\right)\left(\frac{1-b^{-N}}{1+b^{-N}}\right), \tag{4.3}$$

$$I^0_{+\,\text{int1}}(E)=-\frac{|\mu|^2}{2\pi L}\,\text{Im}\,\frac{2ab^{-1}}{(p-1)}\left[\frac{1-b^{-(N-1)}}{1+b^{-N}}\right]^2\times\left\{1-ab^{-1}\left[\frac{1+b^{-(N-2)}}{1+b^{-N}}\right]\right\}^{-1}, \tag{4.4}$$

where $a\equiv a_0$ is given by Eq. (3.20) (with $K=0$), and use has been made of Eqs. (3.8), (3.11), (3.15), (3.16), (3.21)–(3.23), and (3.26). If the influences of higher molecular levels can be neglected, these two terms describe completely the differential spectrum, the contribution $I^K_{+\,\text{int1}}(E)$ representing the effects due to the exciton–exciton interaction. In particular, for $b^{-N}\ll 1$, Eqs. (4.3) and (4.4) reproduce the results by Spano and Manas[33,34] which were obtained when analyzing a system of interacting excitons in the limit of large N.

The two additional terms $I^K_{+\,\text{int2}}(E)$ and $I^K_{+\,\text{high}}(E)$ are defined by Eqs. (3.17)–(3.18), together with Eqs. (3.22)–(3.23) and (3.26) for the Green functions. To simplify the expressions, we note that in the electric-dipole approximation, the energy of resonance coupling $(-L)$ and the coupling parameter χ_α are related to the appropriate transitions dipoles (up to orientational factors) as $L\propto-\mu\mu^*/R^3$ and $\chi_\alpha\propto\mu\mu_{1\alpha}/R^3$. Accordingly, one can write

$$\chi_\alpha=-Ld\mu_{1\alpha}/\mu^*, \tag{4.5}$$

where the parameter d is of the order of unity in the case where μ and $\mu_{1\alpha}$ do not differ significantly in their orientations. It is noteworthy that the relationship (4.5) holds beyond the dipole approximation as well, provided the higher levels α represent the vibrational sublevels of a single electronic state. Under this condition, both the transition dipole $\mu_{1\alpha}$ and the coupling energy χ_α are characterized by the same Condon factors, so one arrives immediately at the relationship (4.5) in which d is some dimensionless parameter. The case accommodates, *inter alia*, a situation where only one higher electronic level (without a vibrational structure) is considered. Such a model has been treated recently by Knoester and Spano[15] in their analysis of the two-photon absorption in a long chain of three level molecules without including the direct exciton–exciton interaction. Using the relationship (4.5), both coefficients u_K and $\widetilde{u_K}$, given by Eq. (3.19), can be expressed via a single function $Q(E)$,

$$\mu u_0=\mu^*\widetilde{u_0}=\frac{d|\mu|^2}{2}Q(E), \tag{4.6}$$

with

$$Q\equiv Q(E)=\sum_\alpha\ \frac{|\mu_{1\alpha}/\mu|^2}{p-1+[\varepsilon_\alpha-2(\varepsilon-2L)]/4L}, \tag{4.7}$$

where $K=0$ is taken in Eq. (4.6), and $p\equiv p(E)$ as in Eq. (3.25). In a similar way, for $K=0$ the coupling parameter (3.20) can be expressed through the same function $Q(E)$,

$$a \equiv a_0 = \gamma/2L + d^2 Q(E)/2. \tag{4.8}$$

The line shape $I^0_{+\,\mathrm{high}}(E)$ given by Eq. (3.18) is also related to the function $Q(E)$, as

$$I^0_{+\,\mathrm{high}}(E) = -\pi^{-1}\frac{|\mu|^2}{4L}\,\mathrm{Im}\;Q(E). \tag{4.9}$$

Finally, the remaining term $I^0_{+\,\mathrm{int2}}(E)$ takes the form,

$$I^0_{+\,\mathrm{int2}}(E) = -\frac{|\mu|^2}{2\pi L}\,\mathrm{Im}\,\frac{d^2Q^2}{4}\,b^{-1}\left[\frac{1+b^{-(N-2)}}{1+b^{-N}}\right] \times\left\{1-ab^{-1}\left[\frac{1+b^{-(N-2)}}{1+b^{-N}}\right]\right\}^{-1}, \tag{4.10}$$

with b as in Eq. (3.27).

The terms (4.3), (4.4), and (4.9)–(4.10) define the full differential spectrum $\Delta I^0(E)$ given by Eq. (4.1). The terms $\Delta I^0_{+\,\mathrm{free\text{-}ex}}(E)$ and $I^0_{+\,\mathrm{high}}(E)$ represent, respectively, contributions due to the free Fermi-excitons and the higher molecular levels. Note that the bleaching contribution (due to the ground state depletion) does not show up in the term $I^0_{+\,\mathrm{high}}(E)$, as the corresponding transition dipoles have been omitted in the transition operator given by Eqs. (3.1)–(3.3). Inclusion of such transition dipoles is straightforward, yet the ground-state absorption to the higher molecular levels is beyond the spectral region of interest and can therefore be disregarded. The other terms $I^0_{+\,\mathrm{int2}}(E)$ and $I^0_{+\,\mathrm{int1}}(E)$ are due to coupling of the Fermi-excitons to the higher molecular levels, as well as due to the direct coupling between the Fermi-excitons. It is noteworthy that the coupling parameter a, Eq. (4.8), entering the line shapes $I^0_{+\,\mathrm{int2}}(E)$ and $I^0_{+\,\mathrm{int1}}(E)$, contains an addition to $\gamma/2L$ which reflects indirect coupling between the Fermi-excitons via the higher molecular levels. The strength of the indirect coupling depends on the function $Q(E)$ generally given by Eq. (4.7). The specific form of the function $Q(E)$ depends on what kind of distribution applies to the energies ε_α of higher molecular states and the corresponding transition dipoles $\mu_{1\alpha}$. For instance, in the case where the transitions to higher levels are distributed according to a Lorentzian centered at $\varepsilon^0_{\mathrm{high}}$ and characterized by the width Δ, Eq. (4.7) simplifies to

$$Q \equiv Q(E) = -\frac{|\mu_{\mathrm{high}}/\mu|^2}{x - \Delta\varepsilon^0_{\mathrm{high}}/4L - i\Delta/4L}, \tag{4.11}$$

where

$$\Delta\varepsilon^0_{\mathrm{high}} = [\varepsilon^0_{\mathrm{high}} - 2(\varepsilon - 2L)] \tag{4.12}$$

is the detuning energy, and the quantity

$$x = [E - (\varepsilon - 2L)]/4L \tag{4.13}$$

is the energy (in $4L$ units) calculated from the bottom of the exciton zone.

Figures 1–5 show plots of the relative pump–probe spectrum

$$y = 4L\Delta I^0(E)/|\mu|^2 \tag{4.14}$$

vs the relative energy x, calculated using the Lorentzian distribution (4.11) for $Q(E)$. Figure 1 gives the spectra for small (a), medium (b), and large (c) values of the relative

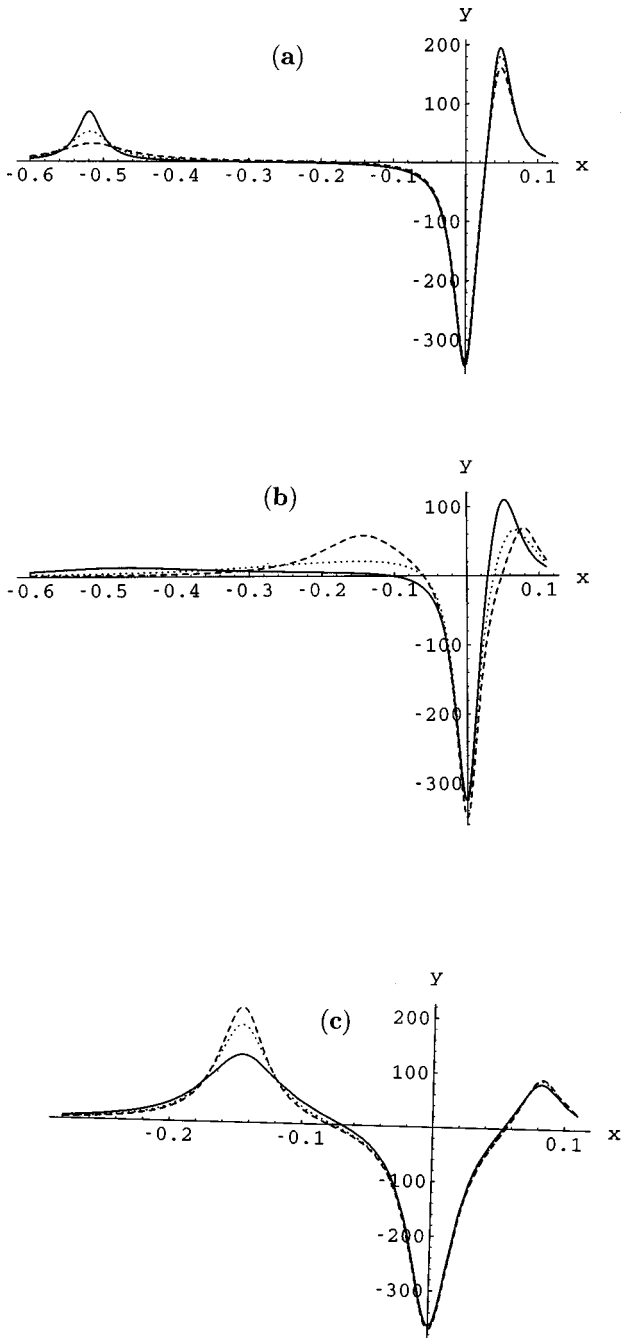

FIG. 1. Relative differential spectrum y vs relative energy x for $N=12$, $\gamma/2L=1.7$, $\Delta\varepsilon^0_{\mathrm{high}}=0$, $\mu_{\mathrm{high}}/\mu=d=1$ and $s=0.02$. The relative widths $\Delta/4L$ are (a) 0.02 (solid line), 0.05 (dotted line), 0.1 (dashed line); (b) 0.3 (solid line), 1 (dotted line), 3 (dashed line); (c) 10 (solid line), 30 (dotted line), 100 (dashed line).

width $\Delta/4L$ of the distribution of higher molecular levels. In all three cases a value of $\gamma/2L=1.7$ has been used for the direct exciton–exciton coupling. In other words, $\gamma/2L$ exceeds the critical value of 1 which corresponds to the onset of formation of a biexciton (below the exciton band-edge at $x=0$) in the case where the influences of the higher molecular levels can be neglected.[33,34,44] For $\Delta/4L \ll 1$ [Fig. 1(a)], the differential spectrum around the band-edge $-0.15<x<0.15$ exhibits a blue shift of the ground-state absorption positioned at $x=0$, such a shift being familiar from the analysis of noninteracting excitons.[9,10,12,14,21,24] In fact, the

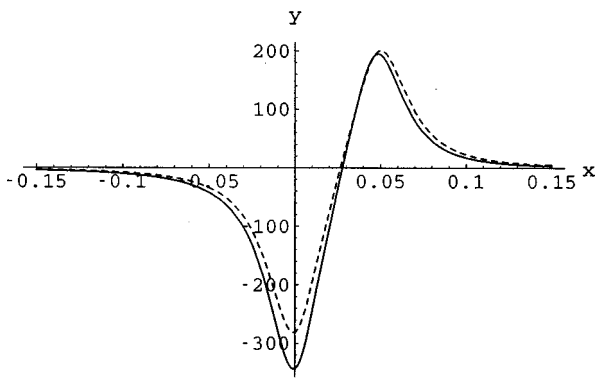

FIG. 2. Exact (solid line) and the approximate (dashed line) differential spectra around the exciton band-edge at $x=0$ for $\Delta/4L=0.02$, $N=12$, $\gamma/2L=1.7$, $\Delta\varepsilon^0_{\rm high}=0$, $\mu_{\rm high}/\mu=d=1$ and $s=0.02$. The approximate spectrum has been calculated using Eq. (4.3) for $\Delta I^0_{\rm free\text{-}ex}(E)$ subject to the replacement $N\rightarrow N_{\rm eff}$. The parameter a featured in Eq. (4.15) for $N_{\rm eff}$ has been calculated at $x=0$ giving $N_{\rm eff}=9.998-0.0799i$.

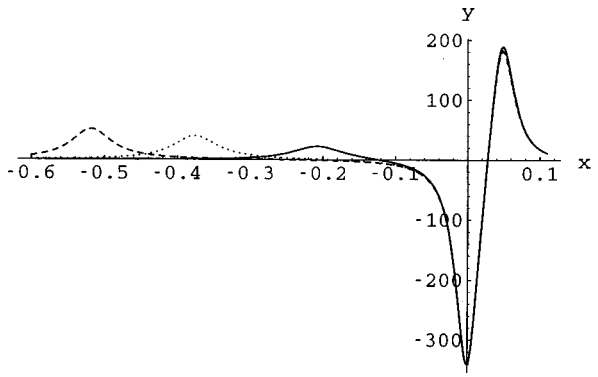

FIG. 3. Relative differential spectrum vs relative energy for $\Delta/4L=0.05$, $N=12$, $\Delta\varepsilon^0_{\rm high}=0$, $\mu_{\rm high}/\mu=d=1$ and $s=0.02$. The parameter $\gamma/2L$ equals -0.5 (solid line), 1 (dotted line), and 1.7 (dashed line).

pump–probe spectrum presented in Fig. 1(a) fits fairly well (at $-0.15<x<0.15$) to the spectrum for the noninteracting Fermi-excitons $\Delta I^0_{\rm free\text{-}ex}(E)$ given by Eq. (4.3), subject to the replacement of the actual size of the aggregate N by the effective one

$$N_{\rm eff}=N+2a/(1-a), \tag{4.15}$$

as illustrated in Fig. 2 for the case where $\Delta/4L=0.02$. Such a replacement has been recently suggested in Ref. 35 analyzing the influence of the exciton–exciton interaction on the optical transitions between the one-exciton and two-exciton states. In the present situation, the concept of the effective number $N_{\rm eff}$ has been extended to include the contribution due to the higher molecular levels into the coupling parameter a. This makes the quantity $N_{\rm eff}$ entering the line shape $\Delta I^0_{\rm free\text{-}ex}(E)$, a complex quantity. Since the widths $\Delta/4L$ are taken to be extremely small in Figs. 1(a) and 2, the coupling parameter a given by Eq. (4.8) acquires a very large imaginary part around $x=0$. As a result, the effective number $N_{\rm eff}$ depends weakly on the magnitude $\gamma/2L$ of the direct coupling, and appears to be close to $N-2$. In other words, the strong indirect coupling between the excitons excludes the two-exciton states containing the excitons at the neighboring sites from the formation of the differential spectrum. In this way, the effective number of molecules contributing to the one- to two-exciton transitions in the spectral area around the exciton band-edge is reduced by 2.[52] For instance, in the situation presented in Fig. 2, one has $N_{\rm eff}=9.998-0.0799i$, i.e., the effective size of the aggregate is reduced from 12 to 10, and a small imaginary part emerges in $N_{\rm eff}$. The approximated spectrum represented by a dashed curve in Fig. 2, fits well the exact result at energies $x>0.02$ corresponding to the excitation by a probe photon of the dissociated two-exciton states. However, at lower energies $x<0.02$ the approximated spectrum underestimates to some extent the contributions due to the induced emission to the ground electronic state, and also the depletion of the ground state absorption, as for both of these spectra the actual number N (rather than the effective one) is more relevant. Note also that despite such an underestimation, the sum rule (3.10) is preserved for the overall differential spectrum, the missing oscillator strength being transferred to the biexciton peak positioned at lower energies.

Figure 1(c) shows another limiting case where the distribution of the higher molecular levels is large compared to the resonance coupling, $\Delta/4L\gg 1$. Here the coupling parameter a is close to $\gamma/2L$, the indirect coupling between the Fermi-excitons providing a small imaginary part to a. This introduces some broadening to the biexciton peak positioned at $x\approx -0.15$ in Fig. 1(c). The linewidth of the biexciton peak increases with decreasing $\Delta/4L$ until the peak becomes almost unresolvable in the case of intermediate widths, $\Delta/4L\sim 1$, as depicted in Fig. 1(b). In this way, the higher molecular levels can broaden considerably the biexciton peaks making it difficult to identify them in the pump–probe spectra. Decreasing further the parameter $\Delta/4L$, one returns back to the limit $\Delta/4L\ll 1$ in which a biexciton peak reappears at much lower energies around $x\approx -0.52$, as shown in Fig. 1(a). It is noteworthy that in the formation of such a biexciton, an important role is played by the indirect interaction between the excitons shifting the biexciton peak additionally downwards from the two-exciton continuum. For instance, in the situation corresponding to Fig. 1(a), the real part of the coupling parameter a calculated at $x=-0.525$ equals approximately 2.6, exceeding substantially the magnitude of the direct exciton–exciton coupling $\gamma/2L=1.7$. It this way, the indirect attraction between the Fermi-excitons allows the formation of a biexciton for $\gamma/2L\leqslant 1$ and even for negative values of the constant $\gamma/2L$, as one can see from Fig. 3 showing the differential spectrum at $\Delta/4L=0.05$ for various values of $\gamma/2L$. A similar effect is known in the theory of biphonons and Fermi resonance in the vibrational spectra of crystals.[47,48] This point was also noted in Ref. 36 analyzing a system of three level molecules without the direct exciton–exciton interaction. On the other hand, for larger relative widths $\Delta/4L$, the onset of biexciton formation depicted in Fig. 4 occurs as usual[33,34,44] at the critical values of $\gamma/2L$ equal to approximately 1, yet the formation of a biexciton is somewhat smoothened by the influences of higher molecular levels (see Fig. 4). Note also that the indirect interaction between the excitons might reduce to some

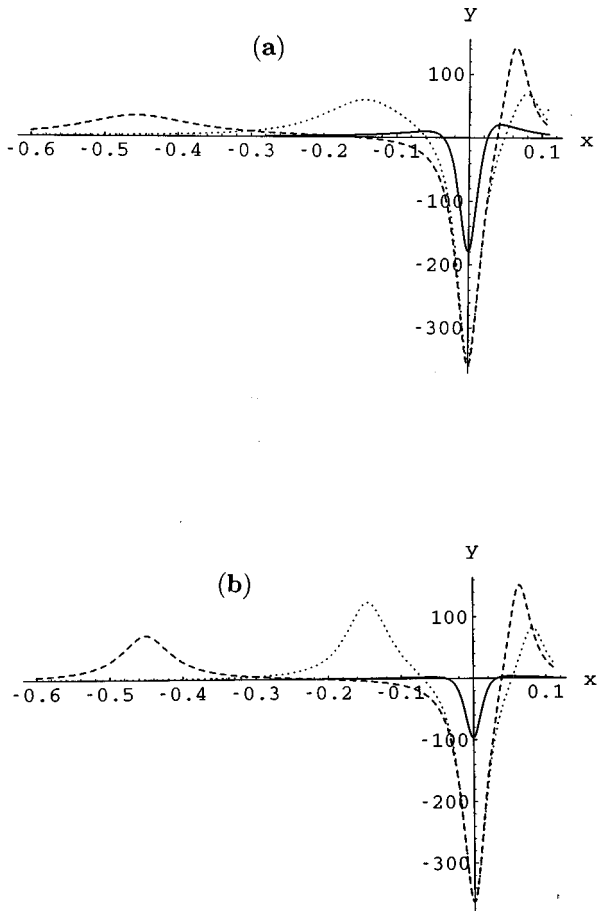

FIG. 4. Relative differential spectrum vs relative energy for $\Delta/4L=3$ (a) and $\Delta/4L=10$ (b), other parameters being $N=12$, $\Delta\varepsilon^0_{\rm high}=0$, $\mu_{\rm high}/\mu=d=1$ and $s=0.02$. In each of these plots the coupling constant $\gamma/2L$ equals 1 (solid line), 1.7 (dotted line) and 2.5 (dashed line).

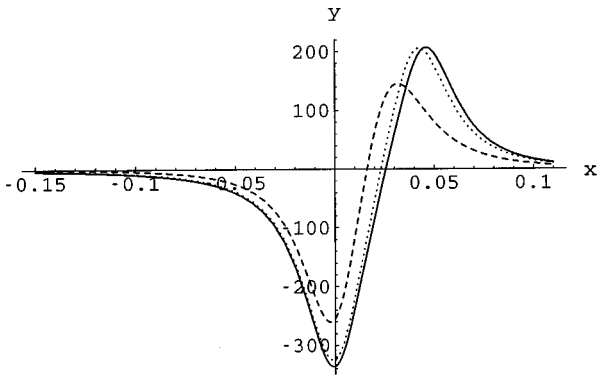

FIG. 5. Relative differential spectrum vs relative energy for $\gamma/2L$ equal to -3 (solid line), -1 (dotted line), and 0.5 (dashed line), other parameters being $\Delta/4L=3$, $N=12$, $\Delta\varepsilon^0_{\rm high}=0$, $\mu_{\rm high}/\mu=d=1$, and $s=0.02$.

extent the critical value for the biexciton formation even in the case of a wider distribution of higher molecular sublevels, provided these sublevels are distributed above the bottom of the two-exciton continuum ($\Delta\varepsilon^0_{\rm high}>0$) thus generating the attractive indirect interaction between the Fermi-excitons. Finally, below the critical values of $\gamma/2L$, the differential spectrum around the band-edge $x=0$ can be once again represented fairly well by the one for noninteracting Fermi-excitons[53] for $\Delta/4L\gtrsim 2$ (see Fig. 5) subject to the substitution of the actual length of the aggregate N by the effective one $N_{\rm eff}$ given by Eq. (4.15).

V. CONCLUSION

The differential pump–probe spectrum has been considered taking into account simultaneously effects of exciton–exciton interaction and of higher molecular levels. The theoretical analysis performed in terms of the Green function technique, provides analytical expressions for the pump–probe spectrum. These expressions are valid for an arbitrary number N of molecules forming the aggregate and any number of molecular states with higher energies, including, *inter alia*, the most common situation in which the higher-lying states are characterized by a dense set of sublevels of electronic, vibrational, etc. origin. The higher levels then play the role of a dissipative system that quenches pairs of lower lying excitons. This makes the exciton–exciton annihilation an irreversible decay process, as usually observed in experiments.[38] In the spectroscopic context, the existence of such a dense set of higher molecular levels introduces widths to biexciton peaks. In some situations [such as the one depicted in Fig. 1(b)] the broadened biexciton peaks become difficult to identify in the pump–probe spectra. In addition, the indirect interaction between the excitons via the higher molecular levels can facilitate the formation of a biexciton at lower than usual values of the direct exciton–exciton coupling γ, in extreme cases even for negative γ values characterizing repulsion rather than attraction between the excitons. It is noteworthy that a similar manifestation of the indirect interaction is known in the theory of biphonons and Fermi resonance in the vibrational spectra of crystals.[47,48] This point was also noted by Knoester and Spano[36] for a system of three level molecules without the direct exciton–exciton interaction. On the other hand, in the region around the exciton band-edge, the pump–probe spectrum exhibits a blue shift of the exciton absorption line for various situations [such as in Figs. 1(a), 2, and 5], the shift being familiar from the analysis of noninteracting excitons.[9,10,12,14,21,24] The differential spectrum can then be described reasonably well in terms of the model of noninteracting excitons, subject to the replacement of the actual number of molecules per aggregate[39] N by the effective one $N_{\rm eff}$ (with $|N_{\rm eff}-N|\ll N$ for sufficiently large aggregates). The latter $N_{\rm eff}$ is shown to be influenced both by the direct coupling between the excitons and by the indirect coupling via the higher molecular levels. In this way, the pump–probe spectroscopy probing the manifold of the two-exciton states and the higher molecular excitations provides information on the effective number $N_{\rm eff}$ that might be somewhat different from N.

ACKNOWLEDGMENTS

The support from the Alexander von Humboldt foundation is gratefully acknowledged. One of us (G.J.) acknowledges J. Knoester for stimulating discussions on the topic during a recent visit by G.J. at the University of Groningen (March–April 1998), as well as Š. Kudžauskas and V. Liuo-

lia for providing Refs. 45 and 46. The authors also thank V. M. Agranovich for comments on the manuscript.

APPENDIX A: DETERMINATION OF THE GREEN OPERATOR

The Green operator in the expression (3.12) for the line shape acts on the excited-state manifold containing either two Fermi-excitons or one excitation with higher-energy. To determine such a Green operator, let us divide the full Hamiltonian (2.6) into the zero-order Hamiltonian and the interaction operator,

$$H=H_0+V \tag{A1}$$

with

$$H_0=H^{\mathrm{ex}}+H^{\mathrm{high}} \tag{A2}$$

and

$$V=H^{\text{high-ex}}+H^{\text{ex-high}}, \tag{A3}$$

where the zero-order Hamiltonians H^{ex} and H^{high} describe, respectively, the subspaces of two-exciton states and higher molecular levels, and the coupling operator V induces transitions between the two sets of states. In a similar way, the Green operator can be represented in terms of its components as

$$G=G^{\mathrm{ex}}+G^{\mathrm{high}}+G^{\text{ex-high}}+G^{\text{high-ex}}. \tag{A4}$$

Applying the left and right Dyson equations

$$G=G_0+G_0VG;\quad G=G_0+GVG_0 \tag{A5}$$

the components $G^{\text{high-ex}}$, $G^{\text{ex-high}}$, and G^{high} of the full Green operator G can be expressed in terms of its projection G^{ex} onto the subspace of the two-exciton states. As a result, the Green operator (A4) can be represented as

$$G=G_0^{\mathrm{high}}+(1+G_0^{\mathrm{high}}H^{\text{high-ex}})G^{\mathrm{ex}}(1+H^{\text{ex-high}}G_0^{\mathrm{high}}), \tag{A6}$$

where G_0 is the zero-order Green operator,

$$G_0\equiv G_0(E+E_K)=[(E+E_K)-H_0-is]^{-1}\quad (s\to+0), \tag{A7}$$

G_0^{ex} and G_0^{high} being its projections onto the subspaces of the two-exciton states and the higher molecular levels, respectively.

To determine the component G^{ex}, we shall substitute recursively the left-hand side of one of the Dyson equations (A5) into its right-hand side, projecting the resulting equation onto the subspace of the two-exciton states. As a result, one arrives at a closed equation for G^{ex}, the solution of which reads

$$G^{\mathrm{ex}}\equiv G^{\mathrm{ex}}(E+E_K)$$
$$=[(E+E_K)-H_{\mathrm{eff}}^{\mathrm{ex}}-is]^{-1}\quad (s\to+0), \tag{A8}$$

where

$$H_{\mathrm{eff}}^{\mathrm{ex}}=H^{\mathrm{ex}}+H^{\text{ex-high}}G_0^{\mathrm{high}}H^{\text{high-ex}} \tag{A9}$$

is the effective Hamiltonian for the two-exciton subsystem. The second term in Eq. (A9) represents the indirect interaction between the Fermi-excitons due to the other subsystem. Using Eqs. (2.13), (2.18)–(2.20), (A2), and (A7), the effective Hamiltonian (A9) can be written explicitly as

$$H_{\mathrm{eff}}^{\mathrm{ex}}=\sum_{\tilde{k}}\ E_{\tilde{k}}b_{\tilde{k}}^{+}b_{\tilde{k}}-\sum_{K}\ \gamma_K'B_K^{+}|g\rangle\langle g|B_K, \tag{A10}$$

with

$$\gamma_K'\equiv\gamma_K'(E)=\gamma-4\cos^2(K/2)\sum_{\alpha}\ \frac{|\chi_\alpha|^2}{E+E_K-\varepsilon_\alpha-is}, \tag{A11}$$

where the second term in Eq. (A11) describes the additional (indirect) coupling between the excitons via the the higher molecular levels. Obviously the effective Hamiltonian (A10) has the same form as the original Hamiltonian (2.13) for the exciton subsystem subject to the replacement $\gamma\to\gamma_K'$. In other words, both direct and indirect interactions between the excitons are characterized by the same combination of the two-exciton operators B_K and B_K^{+}. This will facilitate the subsequent analysis. Note also that the operator B_K, when acting on the state-vectors containing two Fermi-excitons, can produce only the ground state-vector $|g\rangle$. Therefore, insertion of the projection operator $|g\rangle\langle g|$ into the coupling term has no effect on the effective Hamiltonian (A10).

Introducing the Green operator for free excitons

$$G_{\mathrm{free}}^{\mathrm{ex}}\equiv G_{\mathrm{free}}^{\mathrm{ex}}(E+E_K)$$
$$=\left[(E+E_K)-\sum_{\tilde{k}}\ E_{\tilde{k}}b_{\tilde{k}}^{+}b_{\tilde{k}}-is\right]^{-1}\quad (s\to+0), \tag{A12}$$

one can relate it to the full Green operator G^{ex} for the exciton subsystem via the effective Dyson equation,

$$G^{\mathrm{ex}}=G_{\mathrm{free}}^{\mathrm{ex}}-G_{\mathrm{free}}^{\mathrm{ex}}\left(\sum_{K}\ \gamma_K'B_K^{+}|g\rangle\langle g|B_K\right)G^{\mathrm{ex}}, \tag{A13}$$

giving

$$G^{\mathrm{ex}}=G_{\mathrm{free}}^{\mathrm{ex}}-\sum_{K}\ \frac{G_{\mathrm{free}}^{\mathrm{ex}}B_K^{+}|g\rangle\,\gamma_K'\langle g|B_KG_{\mathrm{free}}^{\mathrm{ex}}}{1+\gamma_K'\langle g|B_KG_{\mathrm{free}}^{\mathrm{ex}}B_K^{+}|g\rangle}, \tag{A14}$$

where the solution (A14) has been obtained by taking advantage of the local character[50,54] of the perturbation featured in Eqs. (A10) and (A13). Equations (A6) and (A14) determine the full Green operator G in terms of the Green operator of free excitons $G_{\mathrm{free}}^{\mathrm{ex}}$.

Finally, since

$$J_+|K\rangle=N^{-1/2}\sum_{k}\ b_{K/2+k}^{+}b_{K/2-k}^{+}|0\rangle\cot(K/4-k/2), \tag{A15}$$

we shall write down explicitly the matrix elements of $G_{\mathrm{free}}^{\mathrm{ex}}$ entering Eqs. (3.14)–(3.17) of the main text,

$$\langle K|J_-G_{\mathrm{free}}^{\mathrm{ex}}J_+|K\rangle$$
$$=\frac{1}{N}\sum_{k}\ \frac{\cot^2(K/4-k/2)-\cot(K/4-k/2)\cot(K/4+k/2)}{E+E_K-E(K,k)-is}, \tag{A16}$$

$$\langle K|J_- G^{\rm ex}_{\rm free} B^+_K|g\rangle$$
$$= -\langle g|B_K G^{\rm ex}_{\rm free} J_+|K\rangle$$
$$= \frac{1}{N}\sum_k \frac{[\exp(ik)-\exp(-ik)]\cot(K/4-k/2)}{E+E_K-E(K,k)-is}, \quad \text{(A17)}$$

$$\langle g|B_K G^{\rm ex}_{\rm free} B^+_K|g\rangle = \frac{1}{N}\sum_k \frac{1-\exp(-2ik)}{E+E_K-E(K,k)-is}, \quad \text{(A18)}$$

where

$$E(K,k)=E_{K/2+k}+E_{K/2-k}=2\varepsilon-4L\,\cos(K/2)\cos(k) \quad \text{(A19)}$$

is the energy for a pair of noninteracting excitons, and use has been made of Eqs. (2.15) and (A12).

APPENDIX B: CALCULATION OF THE SUM $S_N(P)$

The sum (3.24) can be rewritten as

$$S_n(p)=\frac{2}{bN}\sum_k \frac{\exp(ikn)}{[1-b^{-1}\exp(ik)][1-b^{-1}\exp(-ik)]}, \quad \text{(B1)}$$

with b as in Eq. (3.27), the sign of the square root being chosen in such a way that $|b|>1$. Representing the denominators in terms of the geometrical progressions, one has

$$S_n(p)=\frac{2}{bN}\sum_k \sum_{r=0}^{\infty}\sum_{p=0}^{\infty} e^{ik(n+r-p)}b^{-(r+p)}. \quad \text{(B2)}$$

The summation over the relative wave vector k covers a set of values defined by Eq. (2.16) (in which $q=1$, as we are dealing with the two-exciton states). As a result, only the terms with $n+r-p=Nm$ contribute to the sum, where m take integer values, giving

$$S_n(p)=2b^{-1}\sum_{m=-\infty}^{\infty}\sum_{r=0}^{\infty}\sum_{p=0}^{\infty} e^{i(KN/2+\pi)m}b^{-(r+p)} \times \delta_{n+r-p,Nm}. \quad \text{(B3)}$$

Here $K=2\pi l/N$ is the full wave vector of the two excitons featured in Eq. (2.16), i.e., at this stage we do not restrict ourselves to the specific case $K=0$ corresponding to $l=0$.

Since $0<n<N$, the summation over m can be split into the part with $m<1$ and that with $m>0$ as

$$S_n(p)=2b^{-1}\left[\sum_{m=0}^{-\infty}\sum_{r=0}^{\infty} e^{i(KN/2+\pi)m}b^{-(2r-Nm+n)} + \sum_{m=1}^{\infty}\sum_{p=0}^{\infty} e^{i(KN/2+\pi)m}b^{-(2p+Nm-n)}\right]. \quad \text{(B4)}$$

Performing summations over m and r (and over m and p), one arrives at the final result for $S_n(p)$,

$$S_n(p)=\frac{2}{b-b^{-1}}\,\frac{b^{-n}-b^{-(N-n)}e^{iKN/2}}{1+b^{-N}e^{iKN/2}}. \quad \text{(B5)}$$

In the case where l is even (e.g., $l=0$ which corresponds to $K=0$), the above result reduces to Eq. (3.26).

[1] E. G. McRae and M. Kasha, in *Physical Processes in Radiation Biology*, edited by L. Augenstein, R. Mason, and B. Rosenberg (Academic, New York, 1964), p. 23.
[2] J. S. Briggs and A. Herzenberg, Mol. Phys. **21**, 865 (1971); J. S. Briggs, Z. Phys. Chem., Neue Folge **75**, 214 (1971).
[3] P. Reineker, *Exciton Dynamics in Molecular Crystals and Aggregates: Stochastic Liouville Equation Approach: Coupled Coherent and Incoherent Motion, Optical Line Shapes, Magnetic Resonance Phenomena* (Springer, Berlin, 1982).
[4] E. W. Knapp, Chem. Phys. **85**, 73 (1984).
[5] P. O. J. Scherer and S. F. Fisher, Chem. Phys. Lett. **86**, 269 (1984).
[6] A. M. Jayannavar, P. Reineker, and B. Kaiser, Z. Phys. B **77**, 229 (1984).
[7] V. Kraus and P. Reineker, Phys. Rev. A **43**, 4182 (1991).
[8] P. Reineker, Ch. Warns, Th. Neidlingen, and I. Barvik, Chem. Phys. **177**, 715 (1993).
[9] G. Juzeliūnas, Liet. Fiz. Rink. **27**, 261 (1987) [English translation, Sov. Phys. Collect. **27**, 7 (1987)].
[10] G. Juzeliūnas, Z. Phys. D **8**, 379 (1988).
[11] F. C. Spano and S. Mukamel, Phys. Rev. A **40**, 5783 (1989).
[12] V. I. Novoderezhkin and A. P. Razjivin, FEBS Lett. **330**, 5 (1993).
[13] J. Knoester, J. Chem. Phys. **99**, 8466 (1993).
[14] F. C. Spano and J. Knoester, in *Advances in Magnetic and Optical Resonance*, edited by W. S. Waren (Academic, New York, 1994), Vol. 18, p. 117.
[15] J. Knoester and F. C. Spano, Phys. Rev. Lett. **74**, 2780 (1995).
[16] S. Mukamel, *Principles of Nonlinear Optical Spectroscopy* (Oxford University Press, New York, 1995).
[17] L. D. Bakalis and J. Knoester, J. Chem. Phys. **106**, 6964 (1997).
[18] E. Gaižauskas and L. Valkūnas, J. Phys. Chem. **101**, 7321 (1997).
[19] V. Malyshev, H. Glaeske, and K.-H. Feller, Opt. Commun. **140**, 83 (1997).
[20] T. Meier, V. Chernyak, and S. Mukamel, J. Phys. Chem. B **101**, 7332 (1997).
[21] T. Ritz, X. Hu, A. Damjanovic, and K. Schulten, J. Lumin. **76&77**, 310 (1998).
[22] R. Gadonas, R. Danielius, A. Piskarskas, and S. Rentsch, Izv. Akad. Nauk SSSR Fiz. **47**, 2445 (1983) [English translation, Bull. Acad. Sci. USSR, Phys. Ser. **47**, 151 (1983)].
[23] R. Gadonas, R. Danielius, A. Piskarskas, T. Gillbro, and V. Sundström, in *Ultrafast Phenomena in Spectroscopy*, edited by Z. Rudzikas, A. Piskarskas, and R. Baltramiejūnas (World Scientific, Singapore, 1988), p. 411.
[24] H. Fidder, J. Knoester, and D. A. Wiersma, J. Chem. Phys. **98**, 6564 (1993).
[25] A. E. Johnson, S. Kumazaki, and K. Yoshihara, Chem. Phys. Lett. **211**, 511 (1993).
[26] K. Minoshima, M. Taiji, K. Misawa, and T. Kobayashi, Chem. Phys. Lett. **218**, 67 (1994).
[27] V. F. Kamalov, I. A. Struganova, Y. Koyama, and K. Yoshihara, Chem. Phys. Lett. **226**, 132 (1994).
[28] M. van Burgel, D. A. Wiersma, and K. Duppen, J. Chem. Phys. **102**, 20 (1995).
[29] J. Moll, S. Daehne, J. R. Durrant, and D. A. Wiersma, J. Chem. Phys. **102**, 6362 (1995).
[30] A. Yu. Borisov, R. V. Gadonas, R. V. Danielius, A. S. Piskarskas, and A. P. Razjivin, FEBS Lett. **138**, 25 (1982); A. P. Razjivin, R. V. Danielius, R. V. Gadonas, A. Yu. Borisov, and A. S. Piskarskas, *ibid.* **143**, 40 (1982); R. V. Danielius, A. P. Mineyev, and A. P. Razjivin, *ibid.* **250**, 183 (1989).
[31] T. Pullerits, M. Chachisvilis, and V. Sundström, J. Phys. Chem. **100**, 10787 (1996); M. Chachisvilis, T. Pullerits, W. Westerhuis, C. N. Hunter, and V. Sundström, J. Phys. Chem. B **101**, 7275 (1997).
[32] H. Ezaki, T. Tokihiro, and E. Hanamura, Phys. Rev. B **50**, 10506 (1994).
[33] F. C. Spano, Chem. Phys. Lett. **234**, 29 (1995).
[34] F. C. Spano and E. S. Manas, J. Chem. Phys. **103**, 5939 (1995).
[35] G. Juzeliūnas and P. Reineker, J. Chem. Phys. **107**, 9801 (1997); J. Lumin. **76&77**, 429 (1998).
[36] J. Knoester and F. C. Spano, in *J-Aggregates*, edited by T. Kobayashi (World Scientific, Singapore, 1996), p. 111.
[37] R. E. Merrifield, J. Chem. Phys. **31**, 522 (1959).
[38] V. Sundström, T. Gillbro, R. A. Gadonas, and A. Piskarskas, J. Chem. Phys. **89**, 2754 (1988); P. J. Reid, D. A. Higgins, and P. F. Barbara, J. Phys. Chem. **100**, 3892 (1996).
[39] The quantity N may not necessarily represent the physical size of the aggregate, but the coherence length of an exciton in an aggregate, as mentioned earlier (Ref. 10).

[40] P. Jordan and E. Wigner, Z. Phys. **47**, 631 (1928).
[41] D. B. Chesnut and A. Suna, J. Chem. Phys. **39**, 146 (1963).
[42] V. M. Agranovich, *Theory of Excitons* (Nauka, Moscow, 1968) (in Russian).
[43] V. M. Agranovich and M. D. Galanin, *Electronic Excitation Energy Transfer in Condensed Matter* (North–Holland, Amsterdam, 1982).
[44] G. Vektaris, J. Chem. Phys. **101**, 3031 (1994).
[45] E. Montrol, J. Math. Phys. **10**, 753 (1969).
[46] K. Lakatos-Lindenberg, R. P. Hemenger, and R. M. Pearlstein, J. Chem. Phys. **56**, 4852 (1972).
[47] V. M. Agranovich, in *Spectroscopy and Excitation Dynamics of Condensed Molecular Systems*, edited by V. M. Agranovich and R. M. Hochstrasser (North–Holland, Amsterdam, 1983), p. 83.
[48] Yet the present situation is somewhat different from that featured in the theory of biphonons and Fermi resonance (Ref. 47), as excitons and phonons are particles obeying different statistics. Specifically, phonons are bonons while excitons are quasiparticles obeying Pauli-statistics. It is the Pauli statistics of the excitons, which is responsible for the blue shift of the exciton absorption line around the exciton band-edge (Refs. 9, 10, 12–14, 24). Furthermore, the theory of Fermi-resonance in crystals (Ref. 47) is normally restricted to a single molecular vibration with higher frequency; this corresponds to inclusion of only one higher molecular level in our case.
[49] A. S. Davydov, *Theory of Molecular Excitons* (Plenum, New York, 1971).
[50] E. N. Economou, *Green's Functions in Quantum Physics* (Springer, Berlin, 1983).
[51] In this discussion, it is implicitly assumed that $L>0$, where $-L$ is the energy of the resonant coupling between the Fermi-excitons. In such a case, the optically allowed transitions take place to the levels situated at the bottom of the exciton band.
[52] A similar conclusion has been reached by Knoester and Spano (Ref. 15) in their analysis of the two-photon absorption by a chain of three level molecules in the absence of the direct interaction between the excitons ($\gamma=0$). Specifically, it was concluded that ''the two-photon allowed space splits into a chain of length of $N-2$ and a 'dimer' subspace'' in the case where the coupling between the excitons and the higher molecular levels exceed considerably the magnitude of the resonance interaction. In the presented situation [Figs. 1(a) and 2] the coupling between the two subsystems is not so strong, yet an additional indirect attraction between the excitons leads to a similar effect. It is to be pointed out that in calculating Figs. 1(a), 2, and 3, the spectral width of higher molecular levels is taken to be very narrow $\Delta/2L\ll 1$. Such a situation is similar to the model of the three-level molecular chain in which the exciton–exciton interaction is now additionally included.
[53] Brief arguments showing that the differential spectrum should not depend significantly on the magnitude of the exciton–exciton coupling, have been presented already in the original paper by Juzeliūnas (Ref. 10), the issue being explored in more detail recently (Refs. 33–35). Specifically, the calculated pump–probe spectrum (Refs. 33, 34) has appeared to be almost independent of the magnitude of the exciton–exciton coupling (if the latter does not exceed its critical value) in the region of the exciton band-edge, the effect being understood (Ref. 35) in simple terms through the concept of the effective number N_{eff}.
[54] G. Juzeliūnas and D. L. Andrews, Phys. Rev. B **49**, 8751 (1994).